Compensation mechanism for N acceptors in ZnO

Eun-Cheol Lee, Y.-S. Kim, Y.-G. Jin, and K. J. Chang
Department of Physics, Korea Advanced Institute of Science and Technology, Taejon 305-701, Korea
(Received 10 April 2001; published 8 August 2001)

We present a mechanism for the compensation of N acceptors in ZnO through real-space multigrid electronic structure calculations within the local-density-functional approximation. We find that at low N doping levels using a normal N_2 source, O vacancies are the main compensating donors for N acceptors, while N acceptors are compensated via the formation of defect complexes with Zn antisites at high doping levels. When an active plasma N_2 gas is used to increase the N solubility, N acceptors are still greatly compensated by N_2 molecules at oxygen sites and N-acceptor–N_2 complexes, explaining the difficulty in achieving low-resistivity *p*-type ZnO.

DOI: 10.1103/PhysRevB.64.085120 PACS number(s): 71.55.Gs, 61.72.Vv, 61.72.Bb, 61.72.Ji

Recently, zinc oxide (ZnO) has attracted much attention because of wide applications for various devices such as piezoelectric transducers, varistors, optical waveguides, and solar cells.[1] Since ZnO has a direct band gap of 3.3 eV and a large exciton binding energy of 60 meV, this semiconductor has been considered as a promising material for short-wavelength optoelectronic devices. In fact, efficient excitonic UV laser actions have been demonstrated at room temperature.[2,3] Undoped ZnO exhibits intrinsic *n*-type conductivity, and very high electron densities of about 10^{21} cm^{-3} are achievable.[4] On the other hand, it is very difficult to fabricate low-resistivity *p*-type ZnO as for other wide band-gap semiconductors, ZnSe and GaN. Among group-IV acceptors, N is considered to be a shallow *p*-type dopant.[5] However, to our knowledge, no one has succeeded in obtaining *p*-type ZnO using a pure nitrogen source, while two groups have successfully fabricated *p*-type samples by codoping N with H or Ga.[6,7] Thus, N acceptors are strongly compensated in ZnO, while *p*-type ZnSe can be grown using a N_2 plasma source.[8,9] Although several theoretical calculations have been done to explain the compensation of N acceptors in ZnSe,[10–12] no clear explanations have been given for the compensation mechanism in N-doped ZnO.

In this paper, we report the results of first-principles pseudopotential calculations for the compensation mechanism in N-doped ZnO. To find dominant compensating species, we examine native point defects and N-related defects such as N-N complexes and N-acceptor–native-defect complexes. When a normal N_2 gas is used as a doping source, N acceptors are mainly compensated by O vacancies and N_O-Zn_O complexes, resulting in extremely low hole concentrations. Even if an active N_2 plasma is used, it is still difficult to achieve high hole carrier densities due to the compensation by N_2 molecules at O sites and N_O-$(N_2)_O$ complexes, explaining the difficulty in obtaining low resistance *p*-type ZnO.[13,14]

The total energies of native and N-related defects are calculated using the first-principles pseudopotential method within the local-density-functional approximation (LDA).[15] Norm-conserving pseudopotentials are generated by the scheme of Troullier and Martins,[16] and then transformed into a separable form of Kleinman and Bylander.[17] In usual plane-wave calculations, a very large number of plane waves are required to adequately describe the localized nature of the Zn $3d$ and O $2p$ wave functions. To deal with such localized orbitals in the valence shell, we use a real-space multigrid method,[18] which has been very efficient in applications to localized systems such as SiO_2.[19] The Laplacians in Poisson and Kohn-Sham equations are expressed up to the twelfth order, based on a finite difference method.[20] The real-space grids are generated by the $84\times48\times80$ mesh, with the spacings (h) of 0.253, 0.256, and 0.246 a.u., respectively. We test various sets of fine grids up to the effective kinetic energy cutoff [$E_{\text{cutoff}}=(\pi/h)^2$] of 200 Ry, and find the grid spacing of about 0.26 a.u. (corresponding to $E_{\text{cutoff}}=146$ Ry) to be sufficient to ensure total energy convergence and suppress numerical instability. We employ a supercell containing 64 host atoms in the wurtzite structure. The summation of the charge densities over the Brillouin zone is carried out using the Γ point. We relax ionic coordinates until the atomic geometry is optimized, using the conjugate gradient technique.

The formation energy for each charge state of a defect is calculated from the total energy, the chemical potentials μ_i ($i=$ Zn, O, and N) of the constituent elements, and the Fermi energy (μ_e).[21] Including all the defects considered here, defect and hole concentrations are determined by the charge neutrality condition.[21] To describe the stoichiometry of ZnO, we use the stoichiometric parameter λ, lying between 0 and 1 under extreme Zn- and O-rich conditions, respectively. The heat of formation of ZnO is calculated to be 3.68 eV, in good agreement with the experimental value of 3.61 eV. The top of the valence band is referenced to zero to describe defect levels in the band gap.

First we examine native point defects, vacancies (V_O and V_{Zn}), interstitials (Zn_i and O_i), and antisites (Zn_O and O_{Zn}). We find that Zn_i has the lowest energy at an octahedral site for both neutral and positively charged states. The six surrounding Zn atoms move away by 0.2 Å from the octahedral site, reducing repulsive interactions between the interstitial and host Zn atoms. The Zn_i-Zn bond distances lie between 2.48 and 2.59 Å, which are smaller than the values of 2.66 and 2.91 Å for bulk Zn metal. When a Zn atom occupies an O site, the neighboring Zn atoms undergo very large lattice relaxations of 0.4 and 0.6 Å, with the Zn_O-Zn

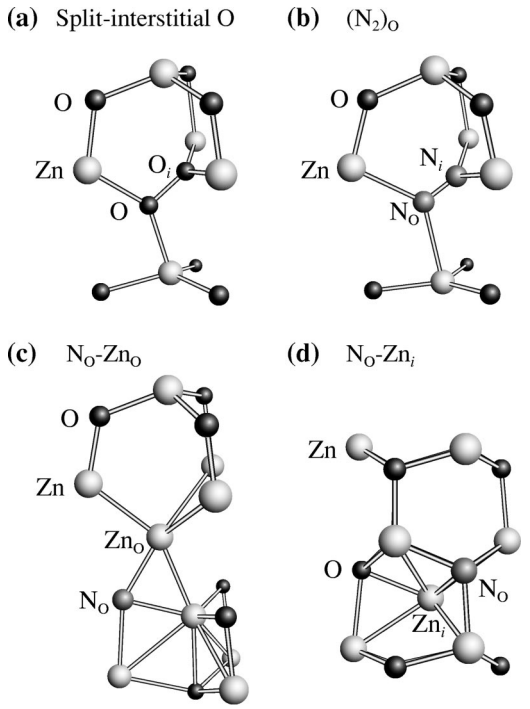

FIG. 1. Atomic structures of the (a) split-interstitial-O_i complex, (b) N_2 molecule at an O site, (c) N-acceptor–Zn-antisite complex, and (d) N-acceptor–Zn-interstitial complex in ZnO.

bond distances of 2.47 and 2.49 Å. For O_i, the octahedral site is lowest in energy for negatively charged states, and the double acceptor level lying close to the valence-band maximum is derived from the empty $2p$ orbital of O_i. On the other hand, for neutral and positively charged states, O_i forms a split-interstitial complex [see Fig. 1(a)] at an O site. In the split-interstitial configuration, each O atom is bonded to two surrounding Zn atoms, and the O_i-O bond is tilted by about 39° from the c axis in the $(2\bar{1}10)$ plane. The split-interstitial complex behaves as a double donor, and its donor level is characterized by the $pp\pi^*$ state of the O_i-O complex, as shown in Fig. 2(a). For a neutrally charged state, since the surrounding Zn $4s$ electrons are transferred to the $pp\pi^*$ level, the O_i-O bond distance is larger by 0.23 Å than that for a free O_2 molecule. Among the native defects, V_O, Zn_i and Zn_O are double donors, becoming possible compensating species for N acceptors, while V_{Zn} and O_{Zn} are double acceptors. The calculated formation energies of native defects are plotted as a function of the Fermi level for both Zn- and O-rich conditions in Fig. 3. Under Zn-rich conditions, V_O is the most stable defect for all the Fermi levels. When the Fermi level is close to the valence-band maximum, V_O, Zn_i, and Zn_O have similar formation energies. On the other hand, in the O-rich limit, V_{Zn} becomes the most stable defect in n-type ZnO, while O_i is energetically more favorable as the Fermi level moves to the valence-band maximum.

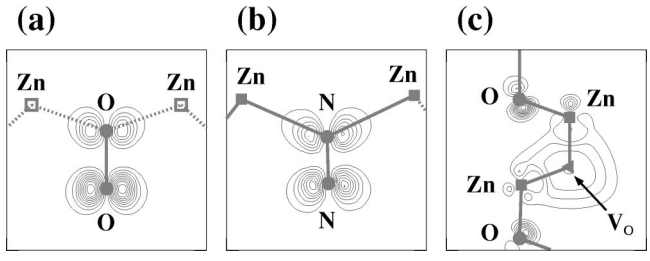

FIG. 2. Charge density contours for the donor levels of the (a) split-interstitial-O_i complex, (b) N_2 molecule at an O site, and (c) O vacancy. In (a), (b), and (c), the contour spacings are 0.01, 0.01, and 0.001 a.u., respectively. The Zn atoms in (a) are located at 0.15 Å below the plane.

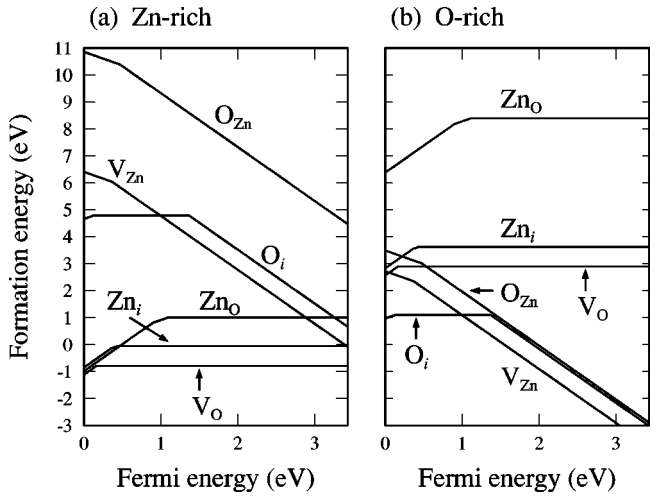

FIG. 3. Defect formation energies as a function of the Fermi level for native defects in ZnO under (a) Zn- and (b) O-rich conditions.

For N-related defects, the calculated formation energies of N_O, $(N_2)_O$, and N_O–double-donor complexes are listed in Table I. Among these defects, N_O is only an acceptor, while the others are donors. When a N_2 molecule is located at an O site, two valence electrons from the nearest Zn atoms occupy the nonbonding state of $(N_2)_O$, as shown in Fig. 2(b). From the analysis of defect transition levels and wavefunctions, we confirm that $(N_2)_O$ acts as a shallow double donor, very similar to the $(N_2)_{Se}$ molecule at a Se site in ZnSe.[12] In the optimum geometry of $(N_2)_O$ [see Fig. 1(b)], the N-N bond is tilted by about 35° from the c axis in the $(2\bar{1}10)$ plane,

TABLE I. Formation energies of N-related defects. The nitrogen chemical potential of $\mu_N = \mu_{N_2}/2$ is chosen, and ΔH is the calculated heat of formation of ZnO. For N-acceptor–double-donor complexes, the binding energies are also given.

Defect	Formation energy (eV)	Binding energy (eV)
N_O	$0.94+\lambda\Delta H$	
N_O^-	$1.41+\lambda\Delta H-\mu_e$	
$(N_2)_O^{2+}$	$-0.78+\lambda\Delta H+2\mu_e$	
$(N_O\text{-}V_O)^+$	$-0.01+2\lambda\Delta H+\mu_e$	0.31
$(N_O\text{-}Zn_i)^+$	$-0.50+2\lambda\Delta H+\mu_e$	1.06
$(N_O\text{-}Zn_O)^+$	$-1.10+3\lambda\Delta H+\mu_e$	1.52
$(N_O\text{-}O_i)^+$	$5.61+\mu_e$	0.60
$[N_O\text{-}(N_2)_O]^+$	$0.35+2\lambda\Delta H+\mu_e$	0.28

similar to the split-interstitial-O_i complex. In this case, the N-N bond length is calculated to be 1.11 Å, which is slightly larger than the calculated value of 1.09 Å for a free N_2 molecule. When N_O forms a complex with a double donor (D) via the reaction

$$N_O^- + D^{2+} \rightarrow (N_O - D)^+ + E_b, \quad (1)$$

where E_b denotes the binding energy, and the N_O-D complex becomes a single donor. The calculated formation and binding energies of various N_O-D complexes are listed for N-rich conditions in Table I. For the N_O-V_O, N_O-$(N_2)_O$, and N_O–split-interstitial-O_i complexes, we find similar binding energies of 0.3–0.6 eV. In the N_O-Zn_O complex [see Fig. 1(c)], the N_O and Zn_O atoms undergo large lattice relaxations of 0.35 and 0.75 Å, as compared to the isolated configuration of N_O and Zn_O. Such large lattice relaxations lead to a large binding energy of 1.52 eV for the N_O-Zn_O complex. For the N_O-Zn_i complex [see Fig. 1(d)], we also find a large binding of 1.06 eV because of the attractive interaction between N_O and Zn_i. A similar large binding energy for this complex was also reported in ZnSe.[11] Among the N_O-D complexes considered here, N_O-Zn_i and N_O-Zn_O have low formation energies in the Zn-rich limit ($\lambda = 0$), compensating efficiently for N acceptors. As going to the O-rich limit, since the formation energies of N_O-Zn_i and N_O-Zn_O increase rapidly, these defects may not be responsible for the acceptor compensation.

To calculate defect and hole concentrations, it is important to know accurate transition levels of donor defects. Since the LDA underestimates the transition levels such as the band gap, corrections are needed for defects that have the characteristics of the conduction band. With the analysis of the angular momentum decompositions, we project the wave functions of defect levels onto the O $2p$ and Zn $4s$ orbitals, which derive the valence-band maximum and conduction-band minimum states, respectively. The defect levels associated with the conduction band are rigidly shifted upwards by the band-gap correction of about 2.5 eV, while those with the valence-band character are assumed to be unaffected. For example, for double donors, the LDA may give rise to errors of about 2.5–5 eV in the formation energies for neutral and $1+$ charge states, while no error is expected for the $2+$ charge state. For both Zn_i and Zn_O, since their donor levels are mainly composed of the Zn $4s$ orbital, lying just above the conduction-band minimum, the band gap correction is needed for the transition levels. Recent experiments[22] showed that Zn_i behaves as a shallow donor, and other LDA and self-interaction-corrected (SIC) pseudopotential calculations[23] also reported that Zn_i and Zn_O are shallow donors. For the split-interstitial O_i, the donor level is characterized by the O $2p$ orbital, corresponding to the $pp\pi^*$ level of O_2, as discussed earlier. Thus, a correction may not be needed for the formation energy of this defect. For V_O, however, we need a special care for the transition level. It was suggested experimentally that V_O is the main source of intrinsic n-type conductivity,[24] while nonlinear spectroscopy measurements showed the donor level at 1.2 eV above the valence-band maximum.[25] Our calculations indicated that the wave function of the V_O defect level is characterized by a combination of the Zn $4s$ and O $2p$ orbitals, as illustrated in Fig. 2(c). Thus, it is more likely that V_O behaves as a deep donor rather than a shallow donor. In fact, we find that the $(2+/0)$ transition level of V_O lies at 0.73 eV below the conduction-band minimum, similar to previous calculations.[26] When we perform the LDA calculations with placing the Zn $3d$ orbitals in the core complex and including nonlinear partial core corrections for the exchange-correlation potential,[27] we still find that V_O acts as a deep donor; the $(2+/0)$ transition level moves from 0.73 to 0.6 eV below the conduction-band minimum, with the band gap increased from 0.9 to 1.7 eV. In this case, since the LDA band gap is still underestimated, the V_O level would be positioned above 1.1 eV from the valence band maximum, if the band-gap correction is included.

In the LDA calculations including the Zn $3d$ electrons as valence states, the severe underestimate of the band gap is attributed to the fact that the semicore Zn $3d$ states are too high, repelling unphysically the occupied p band upward. The failure of the LDA to accurately describe the strongly localized semicore $3d$ states also affects the transition levels and formation energies of defects. Using self-interaction and relaxation-corrected (SIRC) pseudopotentials for InN, Stampfl and co-workers[28] showed that although the single-particle defect level of N_{In} in the band gap is shifted by about 0.5 eV to higher energies, the character of this defect state is very similar, as compared to the LDA results without self-interaction corrections. They also found that valence-band-related defect states are affected in the SIRC calculations, however, the changes of the defect levels are much smaller than the band-gap correction. Recently, Zhang and co-workers[23] have performed the SIC calculations for ZnO, and found that the single-particle defect level of neutral V_O is positioned at 1.0 eV below the conduction-band minimum, close to our LDA calculations. Because of the LDA uncertainty, we calculate defect concentrations by varying the transition level of V_O from 1.1 eV above the valence-band maximum up to the conduction-band minimum. Although defect concentrations depend on the transition level, we find that dominant compensating donors for N acceptors do not change. Thus, we decide to use 1.10 eV above the valence-band maximum for the donor level of V_O, which is close to the experimental value of 1.2 eV, for calculating defect concentrations with the band-gap correction for other donors such as Zn_i and Zn_O.

For all the defects considered here, we estimate defect concentrations under the growth condition using a normal N_2 gas source. Experimentally, the N concentration is controlled by varying the Zn/O flux ratio and the amount of applied N dopants. In our calculations, we simulate these experimental conditions by changing the stoichiometric parameter λ and the nitrogen chemical potential μ_N. The calculated defect and hole concentrations at 1000 K are plotted as a function of the total N concentration in Fig. 4. The N concentration is controlled by the parameter λ, and μ_N is fixed to satisfy the extreme N-rich condition, i.e., $\mu_N = \mu_{N_2}/2$. Then, the calculated hole concentration corresponds to the maximum value

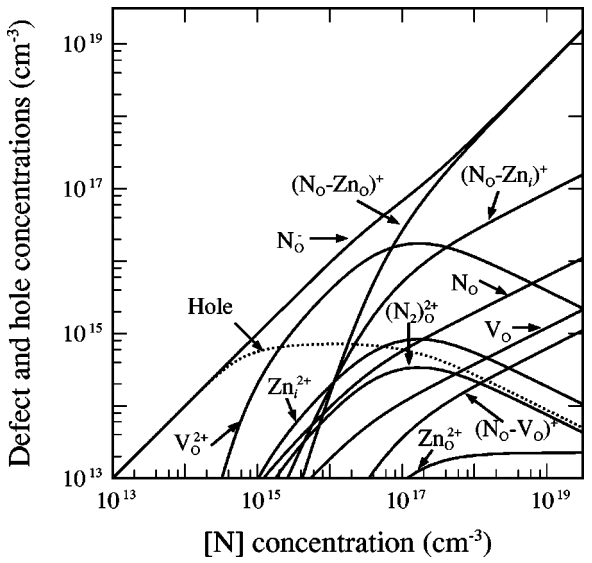

FIG. 4. Defect and hole concentrations as a function of the total N concentration for a normal N_2 gas source. The N concentration is controlled by varying the stoichiometric parameter λ, keeping the N chemical potential in the extreme N-rich limit ($\mu_N = \mu_{N_2}/2$).

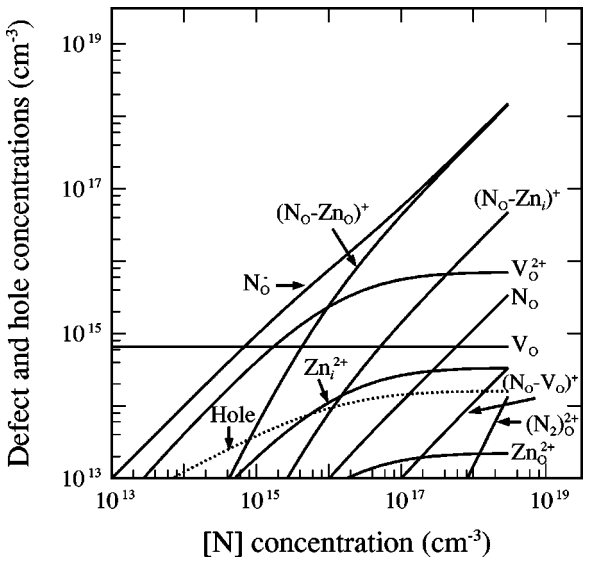

FIG. 5. Defect and hole concentrations as a function of the total N concentration for a normal N_2 gas source. The N concentration is controlled by varying the N chemical potential μ_N, maintaining stoichiometric condition of $\lambda = 0.1$.

achievable under each stoichiometric condition. We find that the N doping is inefficient under O-rich conditions because the total amount [N] of incorporated N impurities is below 8×10^{12} cm^{-3}, which is too small to obtain sufficiently high hole densities. As going to the Zn-rich limit, since the formation energy of N_O decreases significantly, both the hole and N concentrations increase. When the total N concentration lies in the range of 10^{15}–2×10^{17} cm^{-3}, which is achievable under Zn-rich conditions with $\lambda = 0.15$–0.28, the most abundant donor defect is V_O^{2+}. Since the concentrations of split-interstitial O_i, Zn_i, and Zn_O are relatively low, V_O is the dominant compensating species among the donor defects. In this case, the concentration of $(N_2)_O$ is lower by an order of magnitude than that for Zn_i. For high doping levels ([N] $>2\times10^{17}$ cm^{-3} or $\lambda<0.15$), the concentration of $(N_O\text{-}Zn_O)^+$ is similar to that of N_O^- due to the large binding energy. Thus, N_O-Zn_O is the most efficient compensator among the N-acceptor–native-defect complexes in N-doped ZnO. Similarly, previous calculations suggested that N acceptors are compensated by N_{Se}-V_{Se} and N_{Se}-Zn_i complexes in ZnSe.[11] Because of the acceptor compensation, we find that the hole carrier density is saturated to about 2×10^{15} cm^{-3} for N concentrations of 10^{15}–2×10^{17} cm^{-3}, while it decreases as [N] increases further.

We can control the total N concentration by varying μ_N, with keeping the Zn-rich condition of $\lambda = 0.1$; the total N concentration can increase up to 10^{19} cm^{-3}. We find that the hole carrier densities are much smaller than for N acceptors due to the compensation by V_O, as shown in Fig. 5, and eventually saturated to about 5×10^{14} cm^{-3} when the concentration of N_O-Zn_O is close to that of N_O. This behavior is very similar to the results obtained by varying λ. Thus, we conclude that V_O and N_O-Zn_O are the dominant compensating species for low and high doping levels, respectively.

We investigate the *p*-type doping efficiency for a more active N_2 source using a radio frequency or an electron cyclotron resonance plasma. In ZnSe, this doping technique has been very successful in increasing the hole carrier density, as compared to the normal N_2 gas source.[8,9] When an active N_2 source is used, the N solubility increases greatly under O-rich conditions, where native defects and N-acceptor–native-defect complexes are rarely formed; thus, the doping efficiency is expected to increase. To simulate theoretically the active N_2 source, we choose μ_N, which is higher by about 1.5 eV than that for N_2 molecules ($\mu_{N_2}/2$). This N chemical potential is determined by assuming that equal

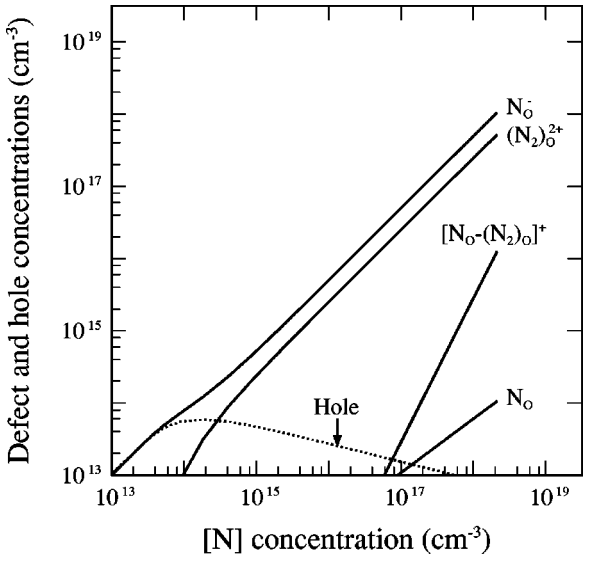

FIG. 6. Defect and hole concentrations as a function of the total N concentration for a plasma N_2 gas source. The N concentration is controlled by varying the N chemical potential μ_N, maintaining a stoichiometric condition of $\lambda = 0.6$.

amounts of N_2 molecules are in the ground and excited states; the energy of an excited N_2 molecule in the $^3\Sigma_u^+$ state is higher by 3.09 eV per N atom, as compared to the ground state ($^1\Sigma_g^+$). We select a suitable O-rich condition of $\lambda = 0.6$, which increases the maximum N concentration from 10^{11} to 7×10^{18} cm^{-3}. As expected, we find that the concentrations of native defects and N-acceptor–native-defect complexes are extremely low, while defects purely composed of N atoms are abundant, as shown in Fig. 6. In this case, the $(N_2)_O$ molecules are the dominant compensating species, with defect densities similar to that for the N acceptors. In ZnSe, it was also shown that $(N_2)_O$ is a major compensating donor for N acceptors.[12] In the O-rich conditions, similarly, the N acceptors are compensated by $(N_2)_O$ and N_O-$(N_2)_O$. We find that the hole carrier density decreases with increasing of [N], with a maximum value of about 2×10^{14} cm^{-3}, as shown in Fig. 6. Thus, it is unlikely to enhance the *p*-type doping efficiency with an active N_2 source, although this N source increases the N concentration. This feature may explain the failure of obtaining low-resistance *p*-type ZnO even if a plasma N_2 source is used.[13,14] In addition, it is difficult to control unintentionally incorporated impurities such as H below the calculated maximum hole concentration of about 10^{15} cm^{-3}, even if a high purity ZnO sample (99.999%) is used. Since water or an H_2 gas is usually present in growing samples, it becomes a source of H. Experimentally, H is known to behave as a donor in ZnO.[29] Recent first-principles calculations also showed that H is a shallow donor, resulting in intrinsic *n*-type conductivity.[30] Thus, the H abundance will be another reason for the difficulty of making high-quality *p*-type ZnO.

In conclusion, we have investigated the compensation mechanism for N acceptors in ZnO through first-principles pseudopotential calculations. We find that for low N concentrations, N acceptors are mainly compensated by O vacancies, while N-acceptor–zinc-antisite complexes becomes the major compensating species as the N concentration increases. Thus, the maximum hole concentration achievable with a normal N_2 source is calculated to be about 10^{15} cm^{-3}. When an active plasma N_2 source is used, although the N solubility increases, the doping efficiency is still low because of the compensation effect by N_2 molecules at O sites and N_O-$(N_2)_O$ complexes.

This work was supported by the supercomputing center in KORDIC, which provided Cray T3E computing times.

[1] F.C.M. Van de Pol, Ceram. Bull. **69**, 1959 (1990).
[2] D.M. Bagall, Y.F. Chen, Z. Zhu, T. Yao, S. Koyama, M.Y. Shen, and T. Goto, Appl. Phys. Lett. **70**, 2230 (1997).
[3] Z.K. Tang, G.K.L. Wong, P. Yu, M. Kawasaki, A. Ohtomo, H. Koinmura, and Y. Segawa, Appl. Phys. Lett. **72**, 3270 (1998).
[4] T. Minami, H. Sato, H. Nanto, and S. Takata, Jpn. J. Appl. Phys., Part 2 **24**, L781 (1985).
[5] A. Kobayashi, O.F. Sankey, and J.D. Dow, Phys. Rev. B **28**, 946 (1983).
[6] K. Minegishi, Y. Koiwai, Y. Kikuchi, K. Yano, M. Kasuga, and A. Shimizu, Jpn. J. Appl. Phys., Part 2 **36**, L1453 (1997).
[7] M. Joseph, H. Tabata, and T. Kawai, Jpn. J. Appl. Phys., Part 2 **38**, L1205 (1999).
[8] R.M. Park, M.B. Troffer, C.M. Rouleau, J.M. DePuydt, and M.A. Hasse, Appl. Phys. Lett. **57**, 2127 (1990).
[9] K. Ohkawa, T. Karasawa, and T. Mitsuyu, J. Cryst. Growth **111**, 797 (1991).
[10] D.B. Laks, C.G. Van de Walle, G.F. Neumark, P.E. Blöchl, and S.T. Pantelides, Phys. Rev. B **45**, 10 965 (1992).
[11] A. Garcia and J.E. Northrup, Phys. Rev. Lett. **74**, 1131 (1995).
[12] B.-H. Cheong, C.H. Park, and K.J. Chang, Phys. Rev. B **51**, 10610 (1995).
[13] Y. Sato and S. Sato, Thin Solid Films **281-282**, 445 (1996).
[14] K. Iwata, P. Fons, A. Yamada, K. Matsubara, and S. Niki, J. Cryst. Growth **209**, 526 (2000).
[15] P. Hohenberg and W. Kohn, Phys. Rev. **136**, B864 (1964); W. Kohn and L.J. Sham, Phys. Rev. **140**, A1133 (1965).
[16] N. Troullier and J.L. Martins, Phys. Rev. B **43**, 1993 (1991).
[17] L. Kleinman and D.M. Bylander, Phys. Rev. Lett. **48**, 1425 (1982).
[18] Y.-G. Jin, J.-W. Jeong, and K.J. Chang, Physica B **273-274**, 1003 (1999).
[19] Y.-G. Jin and K.J. Chang, Phys. Rev. Lett. **86**, 1793 (2001).
[20] J.R. Chelikowsky, N. Troullier, and Y. Saad, Phys. Rev. Lett. **72**, 1240 (1994); J.R. Chelikowsky, N. Troullier, K. Wu, and Y. Saad, Phys. Rev. B **50**, 11 355 (1994).
[21] J.E. Northrup and S.B. Zhang, Phys. Rev. B **47**, 6791 (1993).
[22] D.C. Look, J.W. Hemsky, and J.R. Sizelove, Phys. Rev. Lett. **82**, 2552 (1999).
[23] S.B. Zhang, S.-H. Wei, and A. Zunger, Phys. Rev. B **63**, 075205 (2001).
[24] G.W. Tomlins, J.L. Routbort, and T.O. Mason, J. Appl. Phys. **87**, 117 (2000).
[25] V. Gavryushin, G. Račiukaitis, D. Juodžbalis, A. Kazlauskas, and V. Kubertavičius, J. Cryst. Growth **138**, 924 (1994).
[26] A.F. Kohan, G. Ceder, D. Morgan, and C.G. Van de Walle, Phys. Rev. B **61**, 15 019 (2000).
[27] S.G. Louie, S. Froyen, and M.L. Cohen, Phys. Rev. B **26**, 1738 (1982).
[28] C. Stampfl, C.G. Van de Walle, D. Vogel, P. Krüger, and J. Pollmann, Phys. Rev. B **61**, R7846 (2000).
[29] G. Heiland, E. Mollow, and F. Stöckmann, in *Solid State Physics*, edited by F. Seitz and D. Turnbull (Academic, New York, 1959), Vol. 8, p. 191.
[30] C.G. Van de Walle, Phys. Rev. Lett. **85**, 1012 (2000).